RNA (2000), *6*:1236–1247. Cambridge University Press. Printed in the USA.

Terminating eukaryote translation: Domain 1 of release factor eRF1 functions in stop codon recognition

G. BERTRAM,[1] H.A. BELL,[1] D.W. RITCHIE,[1,2] G. FULLERTON,[1] and I. STANSFIELD[1]

[1]Department of Molecular and Cell Biology, University of Aberdeen, Institute of Medical Sciences, Foresterhill, Aberdeen AB25 2ZD, United Kingdom
[2]Department of Computing Science, University of Aberdeen, Aberdeen AB24 3UE, United Kingdom

ABSTRACT

Eukaryote ribosomal translation is terminated when release factor eRF1, in a complex with eRF3, binds to one of the three stop codons. The tertiary structure and dimensions of eRF1 are similar to that of a tRNA, supporting the hypothesis that release factors may act as molecular mimics of tRNAs. To identify the yeast eRF1 stop codon recognition domain (analogous to a tRNA anticodon), a genetic screen was performed to select for mutants with disabled recognition of only one of the three stop codons. Nine out of ten mutations isolated map to conserved residues within the eRF1 N-terminal domain 1. A subset of these mutants, although wild-type for ribosome and eRF3 interaction, differ in their respective abilities to recognize each of the three stop codons, indicating codon-specific discrimination defects. Five of six of these stop codon-specific mutants define yeast domain 1 residues (I32, M48, V68, L123, and H129) that locate at three pockets on the eRF1 domain 1 molecular surface into which a stop codon can be modeled. The genetic screen results and the mutant phenotypes are therefore consistent with a role for domain 1 in stop codon recognition; the topology of this eRF1 domain, together with eRF1-stop codon complex modeling further supports the proposal that this domain may represent the site of stop codon binding itself.

Keywords: eRF1; protein synthesis; *Saccharomyces cerevisiae*; stop codon; translation termination; yeast

INTRODUCTION

During translation of an mRNA, the newly synthesized protein is released from the ribosome when translocation places a stop codon in the ribosomal A-site. Release factor (RF) proteins direct recognition of the three codons UAA, UAG, and UGA, which signal the termination of polypeptide elongation. In eukaryotes a single release factor, eRF1, decodes all three stop codons (Frolova et al., 1994), whereas prokaryotes employ a pair of so-called class I release factors with overlapping substrate specificity; RF1 decodes UAA and UAG, and RF2 decodes UAA and UGA (Scolnick et al., 1968). In addition, a GTPase superfamily release factor participates in termination; in eukaryotes, this essential factor, designated eRF3, forms a complex with eRF1, and stimulates peptidyl-tRNA hydrolysis once an eRF1/eRF3/ribosome ternary complex is formed (Stansfield et al., 1995a; Zhouravleva et al., 1995; Frolova et al., 1996).

Since the identification of eRF1 as the factor recognizing the stop codon, the precise functions of different domains of eRF1 have gradually been unraveled. The acidic C-terminal residues of the protein constitute an eRF3-binding site (Ito et al., 1998; Eurwilaichitr et al., 1999; Merkulova et al., 1999). The middle domain of eRF1 functions in triggering the ribosomal peptidyltransferase activity, and eRF1 proteins with mutations in the GGQ motif which in vivo are lethal, in vitro are capable of specifically recognizing stop codons and binding the ribosome, but cannot catalyze peptidyl release (Frolova et al., 1999; Song et al., 2000). Only the N-terminal domain of eRF1 has no assigned function, and no domain has yet been identified with a role in stop codon recognition.

Do release factors recognize the stop codon directly? Although a direct role for the ribosome and rRNA in stop codon recognition has been proposed in the past, evidence now points to a direct recognition model for RF stop codon discrimination. First, prokaryote RF2 can be directly UV crosslinked to the stop codon and

Reprint requests to: Ian Stansfield, Department of Molecular and Cell Biology, University of Aberdeen, Institute of Medical Sciences, Foresterhill, Aberdeen AB25 2ZD, United Kingdom; e-mail: i.stansfield@abdn.ac.uk.

downstream nucleotides in vitro, inferring the release factor is in intimate contact with the termination signal (Brown & Tate, 1994; Poole et al., 1998). Second, overexpression of either prokaryote RF1 or eukaryote eRF1 acts to out-compete suppressor tRNA species for stop codon binding. This so-called antisuppressor phenotype indicates both tRNAs and RFs are cognate species in direct competition for stop codon binding (Weiss et al., 1984; Stansfield et al., 1995a; Legoff et al., 1997).

Direct recognition models like these imply that RFs might act in a tRNA-like manner to discriminate between codons. This idea was supported by the discovery that the structure of domain IV/V of elongation factor G complexed with GDP is very similar to that of a tRNA molecule when part of a ternary complex with EF-Tu and GTP, prompting the proposal that protein elongation factors might mimic tRNA molecules (Nissen et al., 1995). On the basis of limited RF sequence similarity to EF-G, the concept of structural tRNA mimicry by the central domain of class I release factors was developed (Ito et al., 1996). The recent solution of the crystal structure of eukaryote eRF1 has allowed a reappraisal of this model for eukaryote RFs, and it is now apparent that, although the central domain of eRF1 at least does not represent a tRNA-like structure (Song et al., 2000), the Y-shaped eRF1 molecule does have both similar shape and overall dimensions to a tRNA. The N-terminal domain 1 of eRF1 may represent a potential anticodon-like region, on the basis of its position relative to the peptidyl-release triggering GGQ motif (analogous to the tRNA CCA acceptor stem; Song et al., 2000). Thus the eRF1-tRNA mimicry model is now supported by direct structural evidence, although it seems likely that the bacterial RFs may be structurally dissimilar to eRF1 because their predicted secondary structures are unalike. It cannot, however, be ruled out that the bacterial RF overall shape may still mimic that of a tRNA. Recently, the crystal structure of another ribosomal A site-interacting protein, the bacterial ribosome recycling factor (RRF), has been solved, revealing it, too, has a tRNA-like shape, and strengthening the tRNA mimicry proposal (Selmer et al., 1999).

How then is stop codon recognition achieved by a tRNA-analog protein RF? In a recent study, mixed RF1/RF2 domain hybrid proteins were constructed and screened for RF1 molecules with RF2-like stop codon specificity. Tripeptide motifs were identified from the central D domain of both release factors that conferred codon specificity, with the first and third amino acids of this peptide discriminating the second and third purine bases of the stop codons (Ito et al., 2000). These findings reinforce the proposal that bacterial RFs directly recognize the stop codon. Eukaryote eRF1 from *Tetrahymena*, recently cloned (Karamyshev et al., 1999), may exhibit natural altered stop codon recognition, as *Tetrahymena* species only recognize UGA as stop, with UAR being reassigned to Gln (Kuchino et al., 1985).

Studies of the class I release factors have thus produced some intriguing clues about how they might act as tRNA analogs to recognize the stop codon, particularly the eRF1 and RRF crystallographic data (Selmer et al., 1999; Song et al., 2000). However, the domain of the eukaryote release factor responsible for this decoding function has not been identified to date. Here we report the use of an in vivo genetic screen for novel eRF1 mutants with unique stop codon decoding properties that define the codon recognition function of a domain on the eRF1 tertiary structure. The findings provide a framework for understanding the fundamental process of how three key genetic code triplets are decoded during protein synthesis, and indicate that essential differences probably exist between eukaryote and prokaryote mechanisms of stop codon recognition.

RESULTS

A novel screen for eRF1 unipotent suppressor mutations specific for one class of stop codon

In *Saccharomyces cerevisiae*, the eRF1 release factor is encoded by the *SUP45* gene (Breining & Piepersberg, 1986), originally identified because *sup45* mutant alleles exhibit a so-called omnipotent suppressor phenotype, capable of suppressing all three stop codons (Hawthorne & Leupold, 1974). Various mechanisms can give rise to eRF1 omnipotent suppression phenotypes, but in essence, the phenotype defines a generally defective release factor, one unable to complex with eRF3 or to associate with the ribosome, or which exhibits disabled stop codon recognition for all three termination codons.

Such omnipotent mutants are not useful tools with which to dissect the mechanism of eRF1 stop recognition. We therefore sought to identify a specific class of eRF1 mutants we designate “unipotent,” wild-type for recognition of two of the stop codons, but exhibiting a suppressor phenotype for the third. In all other respects, the mutants would be capable of wild-type release factor function, and should, in theory, define a stop codon recognition site or domain on the eRF1 molecule. Accordingly, we randomly mutagenized the yeast shuttle vector pGB1, which carries the wild-type *SUP45* gene on its own promoter, using a DNA error repair-defective strain of *Escherichia coli*. This mutant pGB1 library was transformed into yeast strain IS31Δ7b/1c, which carries an otherwise lethal *sup45* gene knockout supported by the *URA3-SUP45*$^{+}$ plasmid pUKC802. A plasmid shuffle strategy (Sikorski & Boeke, 1991) was employed to replace pUKC802 with the pGB1 plasmid library expressing mutant *sup45* alleles (see Materials and methods). The strain also carries three nonsense suppressible alleles, *ade1-14*^{UGA}, *lys2-864*^{UAG}, and *his7-1*^{UAA}, which ordinarily confer auxotrophy for adenine, lysine, and histidine (Chernoff et al., 1994). A total of 50,000 pGB1 library clones in

IS31Δ7b/1c were screened for adenine prototrophy, with lysine and histidine auxotrophy, that is, indicative of a UGA unipotent suppressor phenotype. No examples were isolated of UAG or UAA unipotent suppressors. A total of nine mutants with an *ade1-14* suppressor phenotype were selected for further analysis and designated with allele numbers starting at 700 (Table 1); the mutant pGB1 plasmids were rescued and retransformed into the starting strain to confirm the *sup45* mutant phenotypes. Figure 1 shows the adenine-specific prototrophy phenotypes exhibited by UGA-specific suppressor alleles *sup45-703*, *sup45-702*, and *sup45-731*.

The failure to isolate any UAA or UAG unipotent suppressor alleles in this screen implied that this class of mutant may either be rare, or that unipotent suppressors of this type are naturally weak. Using the same plasmid shuffle protocol, we therefore performed a more sensitive screen of the pGB1 mutant library in another *sup45* disruptant strain, TGB7a/5b, which carries the *ade2-1*^{UAA} and *met8-1*^{UAG} alleles, but also *SUQ5*, a mutant seryl-tRNA. *SUQ5* tRNA has weak UAA nonsense suppressor activity, such that *SUQ5 ade2-1* yeast strains are still auxotrophic for adenine (Cox, 1977). However, an *SUQ5 ade2-1*^{UAA} strain carrying an omnipotent suppressor *sup45* allele is prototrophic for adenine, a so-called allosuppression phenotype (Cox, 1977; Stansfield et al., 1995b). In the presence of a defective release factor complex, *SUQ5* tRNA is also able to weakly suppress UAG amber codons (Stansfield et al., 1995b). The TGB7a/5b strain thus enables more sensitive reporting of both UAA and UAG nonsense suppression. Accordingly, 50,000 pGB1 mutant library clones were screened for a combined methionine prototrophic, but adenine auxotrophic, phenotype, identifying UAG-specific suppressors. Three such mutants were isolated, (designated *sup45-222*, *sup45-228*, and *sup45-242*), and their phenotypes confirmed by rescuing and retransforming the plasmids back into the host strain. No UAA-specific suppressor mutants were isolated from this screen.

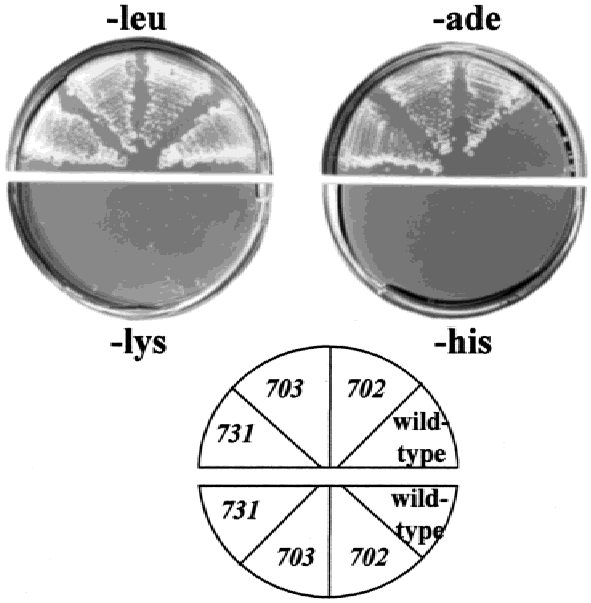

FIGURE 1. A unipotent suppressor screen identifies *sup45* mutants that suppress only one class of nonsense auxotrophic marker. Strain IS31Δ7b/1c, carrying a deletion of the genomic copy of *SUP45*$^{+}$ and the *ade1-14*^{UGA}, *lys2-864*^{UAG}, and *his7-1*^{UAA} mutations, was transformed with either the wild-type *SUP45*$^{+}$ allele or mutant alleles *sup45-702, sup45-703*, or *sup45-731*, carried on plasmid pGB1-*LEU2*. Transformants were plated onto synthetic defined medium lacking either leucine (−leu), leucine and histidine (−his), leucine and lysine (−lys), or leucine and adenine (−ade).

TABLE 1. eRF1 mutations isolated in this study.[a]

sup45 allele	Residue substitution	Nucleotide change
708	I32F	**A**TT → **T**TT
718	P38L	C**C**T → C**T**T
222	M48I	AT**G** → AT**A**
703	V68I	**G**TT → **A**TT
714	V68I, E266E	**G**TT → **A**TT, GA**A** → GA**G**
731	V68A	G**T**T → G**C**T
228	S74F	**A**TC → **T**TC
242	D110G	G**A**C → G**G**C
721	L123V	**T**TG → **G**TG
707	H129R	C**A**T → C**G**T
702	Q415X	**C**AA → **T**AA
709	E428Q	**G**AA → **C**AA

[a]Positions of *sup45* mutants isolated during the course of the two separate screens for unipotent suppressor alleles. The various types of nucleotide transition and transversion are indicated, together with the resultant amino acid changes.

eRF1 mutations identify the function of highly conserved residues within an N-terminal eRF1 structural motif

To establish whether the mutants isolated defined eRF1 amino acid residues within a single domain, the mutations were mapped by sequencing all mutant *sup45* genes on both strands. This revealed that all the mutations, with the exception of *702* and *709*, lay within a region in the N-terminal domain of eRF1 between residue 32 and 129 (Table 1). The results further show that the mutagenesis protocol primarily generated single-point mutations within *SUP45*, both transversions and transitions. The screen appeared to be saturating, because in addition to mutants *703* and *714*, alleles carrying the V68I mutation were isolated a further two times (data not shown).

The mutagenized residues were compared with a multiple alignment of eRF1 amino acid sequences from different phyla, revealing that in all cases the amino acid changes occurred at highly conserved residues within an N-terminal domain that is itself highly conserved (Fig. 2a). Position 68, at which mutations were

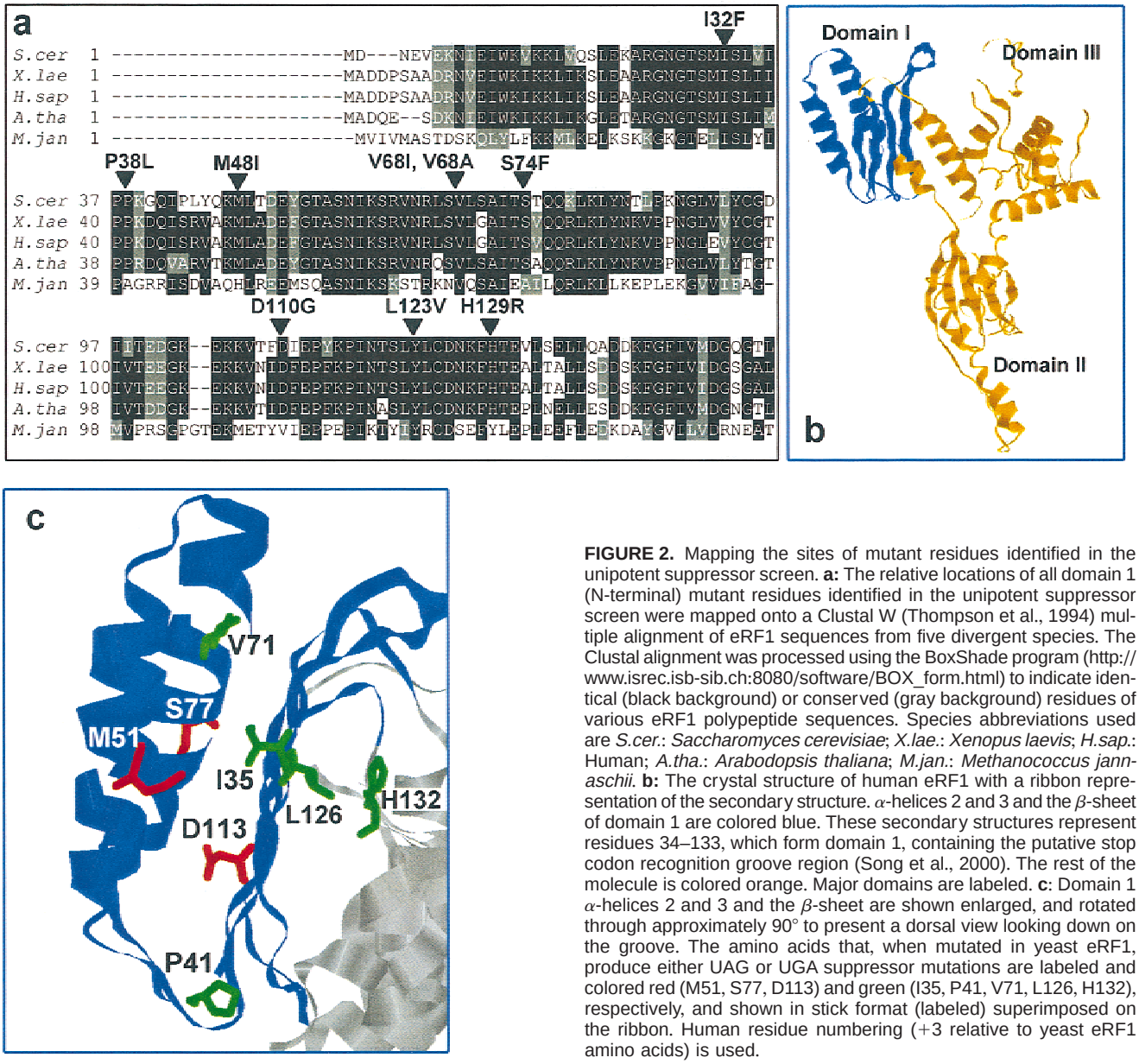

FIGURE 2. Mapping the sites of mutant residues identified in the unipotent suppressor screen. **a:** The relative locations of all domain 1 (N-terminal) mutant residues identified in the unipotent suppressor screen were mapped onto a Clustal W (Thompson et al., 1994) multiple alignment of eRF1 sequences from five divergent species. The Clustal alignment was processed using the BoxShade program (http://www.isrec.isb-sib.ch:8080/software/BOX_form.html) to indicate identical (black background) or conserved (gray background) residues of various eRF1 polypeptide sequences. Species abbreviations used are *S.cer.*: *Saccharomyces cerevisiae*; *X.lae.*: *Xenopus laevis*; *H.sap.*: Human; *A.tha.*: *Arabodopsis thaliana*; *M.jan.*: *Methanococcus jannaschii*. **b:** The crystal structure of human eRF1 with a ribbon representation of the secondary structure. α-helices 2 and 3 and the β-sheet of domain 1 are colored blue. These secondary structures represent residues 34–133, which form domain 1, containing the putative stop codon recognition groove region (Song et al., 2000). The rest of the molecule is colored orange. Major domains are labeled. **c**: Domain 1 α-helices 2 and 3 and the β-sheet are shown enlarged, and rotated through approximately 90° to present a dorsal view looking down on the groove. The amino acids that, when mutated in yeast eRF1, produce either UAG or UGA suppressor mutations are labeled and colored red (M51, S77, D113) and green (I35, P41, V71, L126, H132), respectively, and shown in stick format (labeled) superimposed on the ribbon. Human residue numbering (+3 relative to yeast eRF1 amino acids) is used.

most frequently isolated (V68I or V68A; Table 1) is also conserved in the more diverged eRF1 of archaebacterium *Methanococcus jannaschii* (Fig. 2a).

The mutant residue positions were mapped onto the recently determined tertiary structure of eRF1 (Song et al., 2000). This located the mutant residues at or near the interface between hairpin α-helices 2 and 3, and a β-sheet formed of antiparallel β-strands 1–4 (Fig. 2b,c; Song et al., 2000). On the van der Waals surface of domain 1, this boundary forms a nearly continuous groove. On the basis of the similarity in shape and dimensions between eRF1 and a tRNA molecule, Barford and colleagues have suggested that this domain is likely to perform an anticodon-like role in stop codon recognition (Song et al., 2000). Domain 1 is a similar distance from the eRF1 GGQ motif (responsible for triggering ribosomal peptidyl-transferase activity; Frolova et al., 1999), as that distance between the CCA acceptor stem and anticodon loop of yeast $tRNA^{Phe}$ (Song et al., 2000). The domain 1 putative unipotent suppressor mutants thus lie within the eRF1 structural feature which, on present evidence, is that most likely to represent the release factor stop recognition motif or "anticodon."

The mutant eRF1s exhibit allele-specific bias in efficiency of recognition of individual stop codons

Although the auxotrophy-suppression screens provided a rapid means to identify putative unipotent suppressors, they provide no quantitative information about the

readthrough of the three stop codons in the mutant *sup45* backgrounds. In particular, they do not reveal whether the suppressor mutations are strictly unipotent or whether other stop codons are also readthrough to some extent.

To assess quantitatively the suppression of the three stop codons, we employed a reporter-gene-based assay of nonsense suppression. Separate plasmid constructs were used, in which one of the three stop codons is placed in-frame with the *lacZ* reporter. β-galactosidase expression is thus proportional to stop codon readthrough. *lacZ* expression from these constructs was expressed as a percentage of that measured using a control construct lacking an in-frame stop codon (Stansfield et al., 1995b). To assess the nonsense suppression profiles of mutants isolated from the two genetic screens in a common strain, all the *sup45* suppressor alleles were transformed on plasmid pGB1 into yeast strain IS37/7b [pUKC802], which carried a *sup45* gene knockout and the *SUQ5* ochre suppressor tRNA; plasmid pUKC802 was then shuffled out. The *sup45-708* and *709* alleles could not be shuffled into this strain, for reasons which are unclear. The *lacZ* nonsense suppression assay vectors were used to determine stop codon readthrough in three independent transformants.

The results show that with the exception of UGA readthrough in mutants *222*, *228*, and *242*, which are decreased in comparison to wild-type, to a greater or lesser extent all mutants exhibit increased nonsense suppression of all three stop codons in comparison to a strain dependent upon the wild-type *SUP45*$^+$ allele (Fig. 3A). A cursory assessment of the data therefore defines the mutants simply as omnipotent suppressors. However, considered inspection reveals that the ratios of UAA:UAG:UGA suppression vary between the different mutants. Taking the two extremes, relative to the *SUP45*$^+$ wild-type strain, mutant *228*, isolated as a UAG suppressor, shows approximately 4-fold increases in UAA and UAG respectively, but a 0.42-fold change in UGA readthrough, the latter indicative of antisuppression (Fig. 3B). This pattern of stop codon recognition is completely different from that exhibited by mutant *721*, isolated as a UGA-specific suppressor. UAA and UAG suppression in this mutant is only increased 1.4- and 1.2-fold respective to wild-type, yet UGA suppression is increased 5-fold (Fig. 3B). The *721* readthrough data is therefore consistent with the isolation of this mutant as a suppressor of *ade1-14*^{UGA}, but not *lys2-864*^{UAG} or *his7-1*^{UAA}.

So that this type of comparison can be made for the complete data set, fold increases in stop codon suppression in the mutants relative to wild-type have been calculated (Fig. 3B). Mutant *702* lacks a complete eRF3 interaction domain, and represents an archetypal omnipotent suppressor, in that nonsense suppression arises through an inability to bind the second component of the release factor complex (Ito et al., 1998;

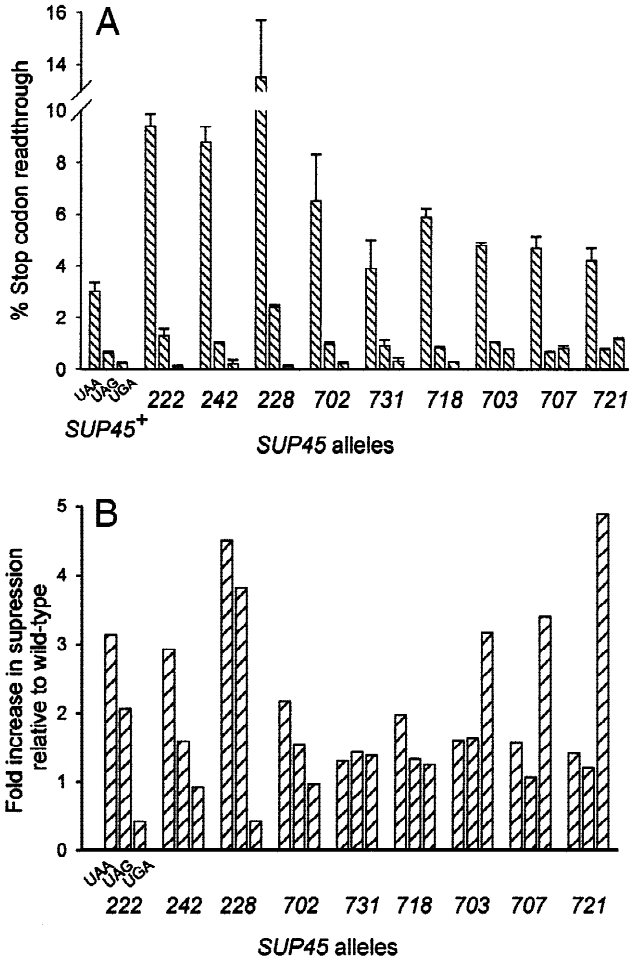

FIGURE 3. Quantitative analysis of the nonsense suppression phenotypes of the domain 1 eRF1 mutants. **A**: Readthrough (nonsense suppression) of all three stop codons was assessed quantitatively using the pUKC815 series vector system (see Materials and methods). Readthrough efficiencies are shown for each stop codon, for the wild-type strain and nine mutants, and represent the average suppression efficiency measured in three independent transformants. Each transformant was assayed in triplicate (variation was typically within $\pm$5%). Error bars represent $\pm$1 standard deviation ($n = 3$) of the average of three independent transformants. **B**: Readthrough efficiencies for the nine mutants were compared to those for the *SUP45*$^+$ wild-type strain. For each mutant, fold increases in suppression of each of the stop codons relative to the same stop codons in the wild-type strain are presented.

Eurwilaichitr et al., 1999); it was therefore used as a benchmark comparison for the other mutants. Examination of the suppression levels, relative to wild-type, for all the mutants reveals three distinct suppression classes (Fig. 3B). Mutants *242*, *731*, and *718* are grouped together as omnipotent, in that their stop codon suppression profiles differ only slightly from that of the C-terminal truncation mutant *702* (Fig. 3B). The second class contains mutants *222* and *228*, isolated as UAG suppressors, and which clearly suppress UAG to a much greater extent than UGA; the latter codon is actually recognized more efficiently than in the wild-type strain. The third class contains mutants *703*, *707*,

and *721*, isolated as UGA suppressors, and which show a much greater increase in UGA suppression than UAG/UAA suppression. It is important to recognize that in the nonsense suppression assay vector system used, the premature stop codons placed in the *lacZ* open reading frame are all in identical contexts (6 nt 5′, and 5 nt 3′ of the stop codon; Stansfield et al., 1995b). Nonsense suppression of each stop codon relative to the other two is thus compared free from context effects.

The domain 1 groove mutants isolated in the two screens thus exhibit definite alterations in their ability to recognize individual termination codons, and strongly support the conclusion that the domain 1 α-helix/β-strand boundary plays a crucial role in stop codon recognition.

Site-directed mutagenesis of residues within the stop-recognition groove region

The mutations identified with stop codon-specific suppressor phenotypes are for the most part single amino acid substitutions of a conservative nature, for example, V68I, L123V, and M48I (Table 1). To confirm first that the mapped mutations were indeed responsible for the phenotypes observed, the V68I mutation (*sup45-703*) was reintroduced into the wild-type *SUP45*$^+$ allele by site-directed mutagenesis. When expressed in strain IS31Δ7b/1c, used in the unipotent suppressor screen, the artificial V68I allele, designated *sup45-V68I.SDM*, conferred an adenine prototrophic and histidine/lysine auxotrophic phenotype, identical to the phenotype of a strain carrying *sup45-703* (data not shown). Quantification of the suppressor phenotype, using the *lacZ* reporter readthrough assay vectors, revealed the suppression profile conferred by *sup45-V68I.SDM* was virtually identical to that of *sup45-703* (Fig. 4).

To test the effect of other amino acid substitutions of a more radical nature in this region of the eRF1 protein, hydrophobic to acidic (V68D) and aromatic to acidic (H129E) substitutions were introduced into the wild-type *SUP45*$^+$ allele. Both these changes were incapable of supporting yeast viability, and in contrast to the wild-type allele or original V68I and H129R *sup45* alleles, these new alleles could not be shuffled into yeast strain IS37/7b [pUKC802] on 5-fluoro-orotic acid medium (5-FOA; Fig. 5). Combining two viable mutations, M48I (*sup45-222*) and D110G (*sup45-242*), which exhibited respectively a UAG suppression biased phenotype and a weak omnipotent suppressor phenotype, in a double mutant, M48I/D110G, also produced a null allele that could not be shuffled into strain IS37/7b [pUKC802] on 5-FOA medium (Fig. 5).

Western blot analysis of eRF1 and eRF3 interaction with the ribosome in the nonsense suppressor eRF1 mutant strains

The eRF1 mutants isolated showed stop codon-biased suppression phenotypes, as a result of mutations in the

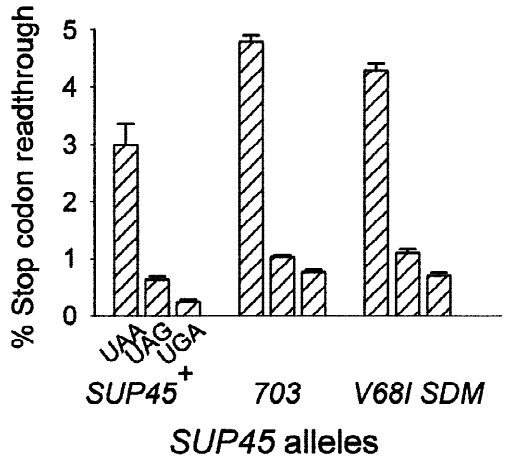

FIGURE 4. Site-directed eRF1 mutant *sup45-V68I.SDM* exhibits an identical profile of stop codon suppression to the original *sup45-703* isolate. Levels of UAA, UAG, and UGA suppression were quantified in strain IS37/7b transformed with either pGB1-*SUP45*$^+$, pGB1-*sup45-703*, or pGB1-*sup45-V68I.SDM*, using the pUKC815 series *lacZ* reporter vectors (see Materials and methods). Three independent transformants were assayed in triplicate. Error bars represent the average of three independent transformants ± 1 standard deviation ($n = 3$).

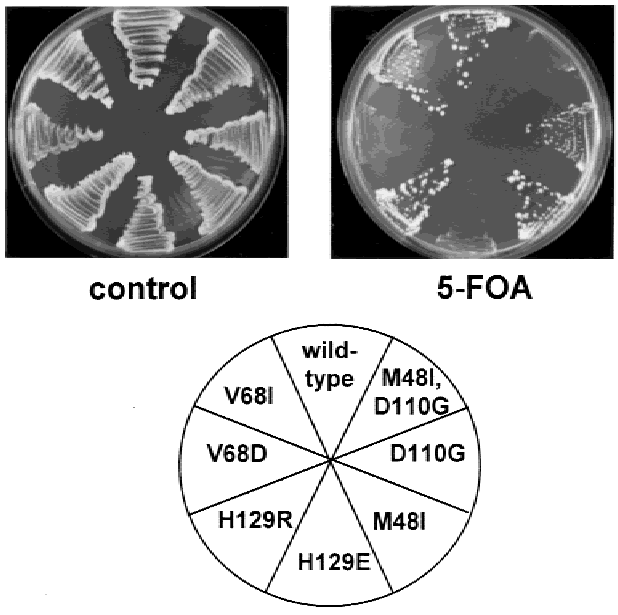

FIGURE 5. Site-directed mutagenesis of eRF1 domain 1. Strain IS37/7b [pUKC802] was transformed with pGB1 vectors expressing mutant eRF1 alleles carrying the following mutations; V68I; V68D (SDM); H129R; H129E (SDM); M48I; D110G; M48I/D110G (SDM). SDM designations indicate the mutations were introduced by site-directed mutagenesis. Transformants were plated out onto either synthetic defined medium minus leucine and uracil (control) or, to shuffle out pUKC802, synthetic defined medium containing 5-fluoro-orotic acid plus uracil minus leucine (5-FOA).

domain 1 groove region. To verify that these phenotypes were caused by defects in the recognition of specific stop codons, it was important to determine that the mutant eRF1 proteins could interact normally with the second component of the release factor complex, eRF3, and that the mutant eRF1s could bind the ribosome normally. This then would exclude two obvious causes for the mutant eRF1 suppressor phenotypes.

Western blots of ribosomal proteins from the wild-type *SUP45* and mutant strains were probed with either anti-eRF1 or anti-eRF3 antibodies (Fig. 6). The results show that with the exception of mutant *707*, none of the mutants showed significant reductions in eRF1–ribosome association; we cannot exclude however the possibility that the *707* mutation, H129R, destroys a major epitope for the anti-eRF1 antibody, causing reduced eRF1 detectability. Mutant *sup45-702* expressed a truncated eRF1 band, consistent with the predicted polypeptide encoded by this nonsense allele with a premature stop codon at position 415. Interestingly, a band representing full-length eRF1 was also present, the result of suppression of the stop codon by mutant eRF1, an effect seen previously with other nonsense alleles of the yeast *sup45* gene (Stansfield et al., 1996). With the exception of *718* and *707*, all the mutants also exhibited wild-type or greater than wild-type levels of eRF3–ribosome association. Together, the western blot data indicate that the majority of eRF1 mutant phenotypes observed are not caused by gross defects in termination complex association with the ribosome.

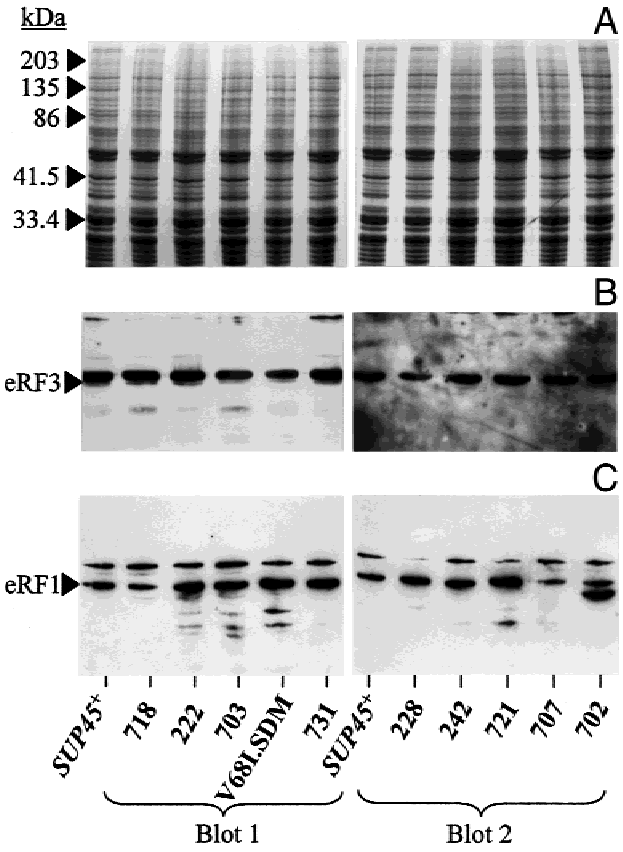

FIGURE 6. Western blot analysis of ribosome-bound eRF1 and eRF3 in the eRF1 mutant strains. Ribosomal fractions were prepared from the *sup45*-disruptant strain IS37/7b supported by either the wild-type *SUP45*$^+$ allele, or each of the mutant alleles. Proteins (25 μg) were separated using SDS-PAGE, and either stained with Coomassie Blue to verify equivalent loadings (**A**), or blotted onto nitrocellulose and probed with anti-eRF3 antibody (**B**), or anti-eRF1 antibody (**C**). Antibody binding was visualized using secondary antibody and chemiluminescent detection (see Materials and methods). The migration positions of molecular mass standards are marked, as are western blot bands corresponding to eRF1 (49 kDa) and eRF3 (79 kDa). The second, heavier (70 kDa) band on the eRF1 western blot is routinely seen using this affinity purified antibody preparation (Stansfield et al., 1992). Western blot samples are split between blot 1 and blot 2, each with its own *SUP45*$^+$ control.

DISCUSSION

The hypothesis that release factors may structurally mimic transfer RNAs has been reinforced by the recent publication of the crystal structures of two A-site interacting factors, eRF1 and the post-termination ribosome recycling factor RRF (Selmer et al., 1999; Song et al., 2000). Here we have strengthened the tRNA-RF mimicry model by the identification of a domain on eRF1 representing a likely candidate responsible for stop codon recognition. *S. cerevisiae* has been used to screen for eRF1 mutants that, although predominantly wild-type for eRF1–eRF3–ribosome complex formation (Fig. 6), nevertheless exhibit some defect in recognition of a subset of the three stop codons (Fig. 3). The mutations identified in this study are all clustered within a small grooved region of eRF1 domain 1, which Barford and colleagues have suggested might represent the stop codon recognition domain because it lies 70 Å from the eRF1 GGQ motif, which promotes peptidyl-release (Frolova et al., 1999; Song et al., 2000). This distance is similar to that separating a tRNA anticodon and the CCA acceptor stem, which triggers peptidyl-transfer. Our analysis of the stop codon suppression profiles of the mutants revealed clear and unambiguous differences in their respective abilities to recognize each of the three stop codons, as would be expected of eRF1 mutants with altered stop codon recognition sites.

Screening for eRF1 unipotent suppressors

Clearly the mutants are not stringent unipotent suppressors, in that they exhibit suppression of all three stop codons; rather they define weak omnipotent suppressors with a bias towards unipotence. Why then were no true unipotent suppressors isolated in either of the two screens? Two explanations are offered; the first is that such eRF1 mutants might be strong suppressors that may not support yeast viability and so were not isolated. A second explanation is that stop codon

recognition by eRF1 might be "holistic"; in other words, a subtle interplay between eRF1 amino acids comprising a stop codon binding site achieves cooperative codon recognition, and a mutation affecting recognition of one stop codon inevitably has consequences for recognition of the other two.

All the mutants exhibit increased UAA suppression to varying degrees. However, we believe our estimates of the true abilities of the mutant eRF1s to recognize UAA were distorted by the presence of the *SUQ5* suppressor tRNA present in the IS37/7b strain background; *SUQ5*, unlike the cell's population of natural suppressor tRNAs, is cognate for UAA, and miscognate for UAG, and so will artificially increase suppression of UAA, and to a lesser extent UAG, above that which would be detected in a wild-type tRNA background. In addition to stop-codon-suppression biased eRF1 alleles, the screens also identified the omnipotent suppressors *sup45-702*, *sup45-718*, and *sup45-731*, although these mutants phenotypically suppressed only the *ade1-14* mutation. Presumably these mutants suppressed *lys2-864*^{UAG} and *his7-1*^{UAA} stop codons weakly. Curiously, mutants *702*, *718*, and *731* also show very low levels of UGA suppression (measured with the *lacZ* reporter system) despite being isolated as *ade1-14* suppressors. This is not because the *ade1-14* premature stop codon is in an easily-suppressed nucleotide context, although context does have important effects on stop recognition by eRF1 in yeast (Bonetti et al., 1995; Mottaguitabar et al., 1998). Sequence analysis of the premature *ade1-14* UGA stop codon identified the mutated codon as TGG (Trp 244) → TGA in the context TTC **TGA** AAC (data not shown), which defines a reasonably good eRF1 substrate (Bonetti et al., 1995; Mottaguitabar et al., 1998).

Modeling a stop codon trinucleotide onto the molecular surface of eRF1 domain 1

The stop codon suppression phenotypes of the mutations, and their colocation on domain 1 of eRF1, support the proposal that this domain has a role in stop codon recognition or may in fact bind the stop codon directly. It was therefore of interest to investigate whether the size of a stop codon trinucleotide and topology of domain 1 is consistent with this role. To test this, the molecular surface of the human eRF1 domain was rendered using the program GRASP (Nicholls et al., 1991). Human and yeast eRF1s are highly conserved in this region (82% identical), and all residues identified through the genetic screens described are identical in the human molecule. Figure 7a shows that there are three obvious topological features, or pockets, identifiable near the α-helix/β-sheet interface of domain 1 that are colocated with a subset of eRF1 suppressor mutations. Pocket 1 is a deep pit lined with hydrophobic residues (L37, I39, V48, and L82), and bounded by residues M51 of α-helix 2 and S123 of the β4-strand. Residue

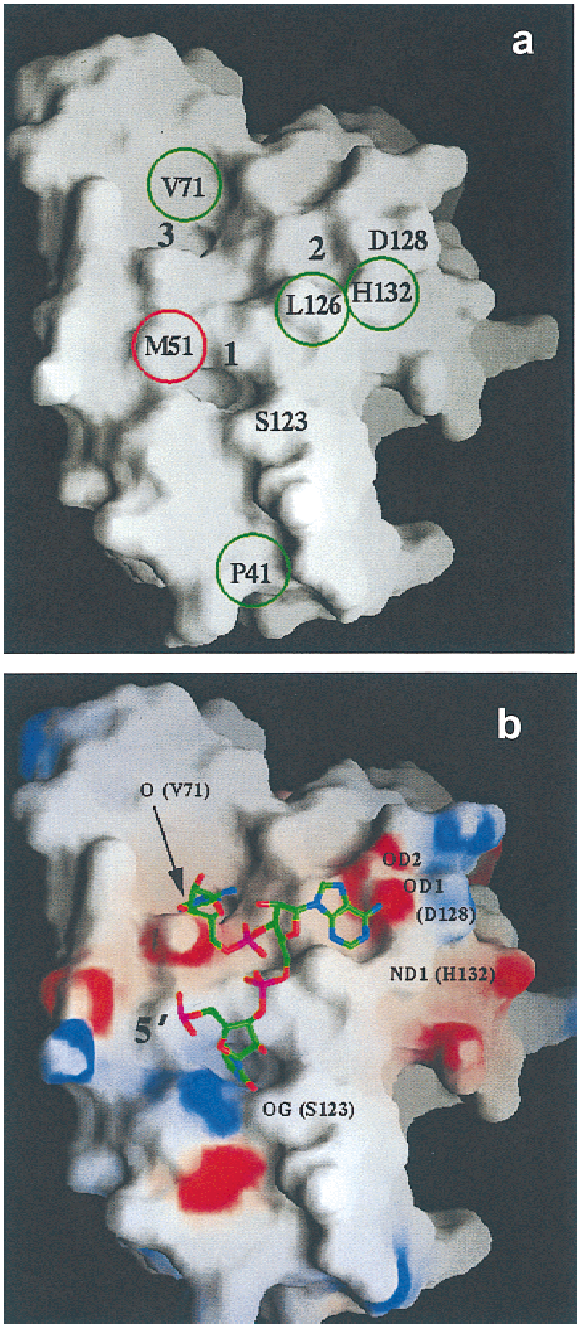

FIGURE 7. Stop codon binding to pockets on the molecular surface of eRF1 domain 1. The molecular surface of human eRF1 domain 1 (Protein Data Bank reference 1DT9) was rendered using the GRASP program (Nicholls et al., 1991). **a**: The potential stop codon binding pockets identified are labeled 1, 2, and 3. The sites of residues P41, M51, L126, H132, and V71 (human numbering), identified in the two unipotent suppressor screens are labeled, as are residues D128 and S123, two potential hydrogen bond donors discussed in the text. Red circles represent residues identified as UAG suppressors and green circles those identified as UGA suppressors. **b**: A UAA stop codon trinucleotide is modeled into pockets 1–3 on the eRF1 domain 1 GRASP-rendered surface. Surface charge is represented in red (−20 mV; negative charges) or blue (+30 mV; positive charges). The approximate positions of potential hydrogen bonded atoms are labeled; δ oxygens 1 and 2 of residue Asp 132 (OD1, OD2); δ nitrogen of His 132 (ND1); γ oxygen of Ser 132 (OG); carbonyl peptide oxygen of Val 71 (O).

M51 corresponds to the M48I mutation in *sup45-222* (human residues are numbered +3 with respect to yeast eRF1 amino acids). Pocket 2 resembles a semicircular bay, made up of residues L126, D128, and H132, and is associated with the yeast L123V and H129R mutations (*sup45-721*, *sup45-707*). As with pocket 1, the lining of pocket 3 is largely hydrophobic in character (I35, L52, A59, V71, V78, C127), but with a potential hydrogen bonding site at the carbonyl oxygen of V71. This pocket is associated with the *sup45-703* V68I and *sup45-708* I32F mutations (human eRF1 residues 71 and 35, respectively). Importantly, four of the five mutant residues showing bias in stop codon recognition map at the three pockets (M48, V68, L123, and H129), and three of the remainder contribute to the stability of the α-helix/β-sheet interface (see below). This indicates that at this interface, the domain 1 pocket region plays an important role in stop codon recognition.

To investigate whether the identified pockets can accommodate a model stop codon, UAA was docked into the putative binding site using a combination of the rigid-body docking program, Hex (Ritchie & Kemp, 2000), and the program Quanta (Molecular Simulations Inc., Burlington, Massachusetts), used to adjust the trinucleotide torsion angles. Best fit models were further refined to produce the model shown in Figure 7b. There are no nonbonded contacts of less than 1.8 Å, yet burial of hydrophobic surfaces is very good and each base can form at least one hydrogen bond with eRF1 (U-O2 with R47 or S123 side chain; A-N6 with D128 side chain; A-N6 with V71 peptide backbone). No other suitable docking orientations could be identified. The model proposed here seems the most likely on the basis of intimacy of fit, and it supports the hypothesis that the three RF pockets may represent the site of stop codon recognition.

eRF1 domain 1 codon specificity; excluding UGG tryptophan codons

If the domain 1 pockets identified do represent the site of eRF1-codon interaction, they should be able to bind all three stop codons, but not the 61 sense codons. The stop codon binding model described can explain such specificity. For example, placing a cytosine in pocket 1 would involve replacing the conjugated uridine carbonyl O4 atom with a much more hydrophilic amino group deep in the hydrophobic pocket, which could disfavor binding. Similarly, placing a small uracil or cytosine base in the large pocket 3 could produce insufficient desolvation of the pocket for binding; placing either of these small bases in pocket 2 would involve the loss of a hydrogen bond with D128. These observations support the notion that a uracil base at the 5′ end of the codon is a requirement for recognition by eRF1, and that pockets 2 and 3 are arranged to accept only purines. Furthermore, we suggest this model can account for the fact that UGG signals tryptophan and not "stop." Our modeling studies have indicated that the nucleotide backbone may be articulated to permit pockets 2 and 3 to accommodate, and hydrogen bond, purines at these positions, for instance by switching pocket 2-base hydrogen bonding from oxygen D1 of D128 to either oxygen D2 of D128 or H132 for the codons UAA, UAG, or UGA (Fig. 8). In other words, the identity of the base at pocket 3 determines which eRF1 atom is used to hydrogen bond the pocket 2 base. However, placing UGG into the eRF1 pockets would involve two opposing backbone articulations, precluding simultaneous formation of hydrogen bonds at pockets 2 and 3, and preventing UGG recognition. Hence, the "articulated coupling" behavior of the nucleotide backbone and the limited hydrogen bonding opportunities of the binding site provide a possible mechanism to explain how eRF1 might specifically bind only the three codons, UAA, UAG, and UGA, and yet exclude the UGG tryptophan sense codon.

The model can also account for phenotypes conferred by the identified domain 1 mutations. Mutations *sup45-707* (H129R) and *703* (V68I) both specifically suppress UGA codons, with UAA and UAG recognition remaining relatively unaffected. We propose that two distinct mechanisms account for these phenotypes. The replacement of His 129 (H132 human numbering) by arginine in mutant *sup45-707* could obstruct hydrogen bonding to the guanine in UGA (Fig. 8), explaining the mutant *707* UGA suppressor phenotype. UAG/UAA recognition by the H132R mutation would be relatively unaffected, as was in fact found, because D128 could still hydrogen bond with a pocket 2 adenine base. Mutant *703* (V68I) illustrates well the principle of articulated coupling between binding pockets. Although Val 71 (human numbering) is located at pocket three, UAA and UAG, despite having different third position bases, are still recognized. We propose that UGA is recognized poorly because the extra methyl group introduced by substituting Ile for Val71 interferes with the exact positioning of third position adenine needed to allow second position guanine to hydrogen bond with

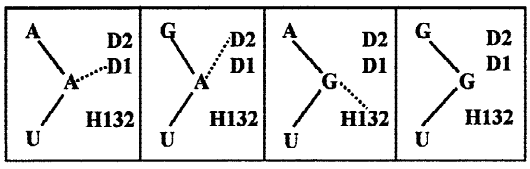

FIGURE 8. A model for eRF1 domain 1 stop codon binding. A possible model for how each of the three stop codons and UGG Trp might be hydrogen bonded at pocket 2, conferring discriminatory ability on the binding pockets. As the identity of base 3 changes, nucleotide backbone articulations dictate alternative hydrogen bonding arrangements at pocket 2. The eRF1 atoms at pocket 2 participating in hydrogen bonds are shown (D1 and D2 are the oxygens of D128). For clarity, the anchoring S123 and V71 hydrogen bonds at pockets 1 and 3 are not shown.

H132. Although the residues of three other mutations, P41L, S77F, and D113G, are located at some distance from the identified pockets, these residues help maintain the correct topology of pockets 1 and 3 by stabilizing the α-helix/β-sheet interface; P41 constrains the α-helix/β-sheet hinge angle, and a pair of hydrogen bonds, S77-N111 and D113-R81, at the "back" of the α-helix/β-sheet interface serve to lock the secondary structural elements into position.

Other proteins are known that bind single-stranded RNA molecules in a sequence-specific manner, most notably the splicing proteins U1A and U2B″. In these ribonucleoprotein interactions, packing of the RNA by hydrophobic amino acids is important (Rimmele & Belasco, 1998), as was found for eRF1, where subtle hydrophobic residue substitutions perturb recognition in a codon-specific manner (pocket 1, M48I; pocket 2, L123V; pocket 3, V68A/I; yeast numbering). The crystal structures of these molecules in complex with their RNA snRNP partners reveals the bound RNA is extensively hydrogen bonded with the U1A protein (Oubridge et al., 1994; reviewed in Draper, 1999), in contrast to the stop codon–eRF1 binding model presented here in which hydrogen bonding opportunities are limited and where sequence recognition of an unstructured RNA molecule is achieved on the principle of articulated coupling between binding pockets. The scarcity of eRF1–stop codon hydrogen bonding is surely a prerequisite for bound molecules that must rapidly dissociate once peptidyl release has been triggered. Second, restricting hydrogen bond opportunities may confer eRF1 stop codon specificity, as outlined above.

Our model for eukaryote eRF1 stop codon recognition is obviously substantially different from that developed for bacterial RFs (Ito et al., 2000). The RF discriminatory tripeptide identified is located in RF domain D at the center of the protein sequence, whereas the mutant screen in this study identified the eRF1 N-terminal domain as important for recognition (Ito et al., 2000). Prokaryote and eukaryote stop codon recognition mechanisms may however be mechanistically dissimilar, because in the bacterial RF, a mutant omnipotent discriminatory tripeptide Ser-Pro-Thr is able to recognize UGG tryptophan in addition to all three stop codons (Ito et al., 2000). The eRF1 omnipotent codon recognition mechanism obviously circumvents this problem, a discrimination ability explained by the model we describe. Another obvious difference between eRF1 and RF1/2 stop recognition is that the three eRF1 nucleotide binding pockets we describe are not part of a compact tripeptide motif recognizing the second and third bases of the stop codon, but instead form from nonadjacent residues brought together by the fold of domain 1. This is perhaps unsurprising, because the substantial differences in predicted secondary structure between RF1/2 and eRF1 argue that these may be structurally distinct polypeptides.

In this study, we present evidence for the identity of an eRF1 domain important for stop codon recognition, based on the phenotypes and locations of a series of novel eRF1 mutants. The eRF1-stop codon complex model presented is consistent with eRF1 domain 1 topology, the mutation analysis, and the stop codon recognition profile of eRF1, and indicates that this domain may represent the site of stop codon recognition itself. The model itself must however be treated with some caution; the temperature (B-) factors of a large proportion of atoms in the eRF1 structure are high, perhaps resulting from their inclusion in the refinement process despite the relatively high R factor/moderate resolution of the structure (free R factor, 31.4%, resolution of 2.7 Å; Song et al., 2000). Nevertheless, although exploratory, the model does place four of the five residues causing biased stop codon suppressor phenotypes at three pockets on the eRF1 surface, into which a stop codon can be modeled and hydrogen bonded. Although no other suitable stop codon binding topology could be found on domain 1, the model will require verification using stop codon eRF1 crosslinking data and or eRF1/stop codon cocrystallization. The results described nevertheless represent a framework for addressing the molecular basis of specific codon recognition by a eukaryote protein release factor.

MATERIALS AND METHODS

Microbial strains and growth conditions

S. cerevisiae strains used in this study were TGB7a/5b (*sup45*::*hisG ade2-1^{UAA} met8-1^{UAG} ura3-52, leu2-3,112* [pUKC802]), IS31Δ7b/1c (*sup45*::*hisG leu2-3,112 ura3-52 ade1-14^{UGA} lys2-864^{UAG} his7-1^{UAA}* [pUKC802]), and IS37/7b (*sup45*::*hisG SUQ5, leu2-3,112, ura3-52, ade2-1^{UAA},met8-1^{UAG}* [pUKC802]; *his3* and *can1-100* not tested). Yeast strain matings and sporulations were carried out according to standard protocols (Sherman & Hicks, 1991). Yeast strains were grown on either YEPD complete medium (2% (w/v) glucose, 2% (w/v) Bacto-peptone, 1% (w/v) yeast extract) or defined minimal medium (0.67% (w/v) Difco defined minimal medium without amino acids, 2% (w/v) glucose) supplemented with the appropriate amino acids and bases. The plasmid shuffling protocol was carried out on medium containing 5-FOA (2% glucose, 0.67% yeast nitrogen base, 0.1% (w/v) 5-FOA, 20 μg/mL uracil; Sikorski & Boeke, 1991).

E. coli strain XL1Blue (*recA1 endA1 gyrA96 thi-1 hsdR17 supE44 relA1 lac [F′ proAB lacI^{q}ZΔM15 Tn10(Tet^r)*) was used throughout for cloning experiments and grown as described (Sambrook et al., 1989).

Plasmid constructs

DNA manipulation and plasmid construction was carried out according to standard protocols (Sambrook et al., 1989). To generate plasmid pGB1, a 2.64-kb *Sal*I/*Xho*I fragment from plasmid pUKC638 (a gift from K.M. Jones and M.F. Tuite,

University of Kent) containing the entire *SUP45* gene and its promoter was cloned into the *Xho*I site of pRS315 (Sikorski & Hieter, 1989). Plasmid pUKC802 (*SUP45-URA3*) is described elsewhere (Stansfield et al., 1992). To generate plasmid pGB4, plasmid pUKC600, containing the entire *SUP45* gene including its promoter on a *Sal*I/*Xho*I fragment in pBluescript (Stratagene), was first cut with *Hin*dIII/*Xba*I. The resulting DNA was treated with Klenow enzyme and religated to generate plasmid pGB2. A 3.8-kb *Bam*HI/*Bgl*II fragment from pNKY51 (American Type Culture Collection; Alani et al., 1987) containing the *hisG-URA3-hisG* "ura-blaster cassette" was subcloned into the *SUP45* coding region in plasmid pGB2 cut with *Bam*HI and *Bgl*II, generating plasmid pGB4.

Construction of a *sup45::hisG* disruption

SUP45 gene disruption using the ura-blaster method was carried out as described (Alani et al., 1987). To disrupt the yeast *SUP45* gene, the 5.0-kb *Xba*I/*Xho*I fragment from pGB4 was purified and used to transform a diploid strain of *S. cerevisiae*. Uracil prototrophs were selected and the disruption was confirmed by PCR on genomic DNA, and by tetrad analysis on the heterozygote disruptant diploid. 5-FOA-containing media was used to resolve the integrated *URA3* marker.

Generation of an eRF1 mutant library and library screening

Plasmid pGB1 (*LEU2, SUP45*) was mutagenized by replication in DNA error-repair defective XLI-Red *E. coli* (Stratagene) according to the manufacturer's instructions. Subsequently, the pGB1 *sup45* mutant library was transformed into either strain TGB7a/5b or IS31Δ7b/1c that contained a genomic *sup45* deletion supported by plasmid pUKC802 (*SUP45*, *URA3*) using standard protocols (Gietz & Woods, 1994). Transformants were replica plated in parallel onto (1) synthetic depleted medium lacking either histidine, lysine, adenine, or methionine and (2) identically depleted medium containing 5-FOA. Transformants that were prototrophic for these nutrients on the 5-FOA medium, but auxotrophic for the supplements on 5-FOA-free medium, were selected for further analysis. This protocol allowed suppression caused by genomic mutations and plasmid-borne *sup45* suppressor mutations to be distinguished.

Plasmid rescue and allele sequencing

Plasmid DNA was recovered from putative positive yeast clones (Hoffman & Winston, 1987) and transformed into *E. coli* XL1-Blue electrocompetent cells (Strategene) by electroporation following the manufacturer's protocol. The entire *sup45* coding sequence from each clone was sequenced on both DNA strands using spaced oligonucleotides, four on each strand.

Site-directed mutagenesis

Site-directed mutagenesis (SDM) was performed using the Stratagene Quickchange™ Site-Directed Mutagenesis Kit according to the manufacturer's protocol. Oligonucleotide primers were designed to incorporate the required base changes and diagnostic restriction endonuclease sites were included that introduced silent mutations. To confirm the SDM changes and to ensure no additional errors had been introduced by PCR, the entire *sup45* allele from each clone was sequenced on both DNA strands as described.

Quantification of nonsense suppression efficiency using β-galactosidase assays

Yeast strains containing mutant alleles of *sup45* were transformed with each of the following vector series, pUKC815/817/818/819 (Stansfield et al., 1995b). β-galactosidase assays were performed as previously described (Finkelstein & Strausberg, 1983). For each combination of mutant and pUKC815-series assay vector, three individual yeast transformants were each assayed in triplicate.

SDS-polyacrylamide gel electrophoresis and Western blot analysis

Ribosomal fractions and postribosomal supernatants were prepared as described previously (Stansfield et al., 1992). SDS-PAGE was performed using 10% (w/v) polyacrylamide gels according to standard protocols (Laemmli, 1970). Proteins were transferred onto nitrocellulose using a semidry blotting apparatus (Bio-Rad) according to the manufacturer's instructions. The blots were probed using either affinity purified anti-eRF1 polyclonal antibody (Stansfield et al., 1992) or anti-eRF3 polyclonal antibody using standard protocols (Harlow & Lane, 1988). Bound antibody was detected using the ECL detection kit (Amersham) according to the manufacturer's protocol.

Cloning of the ade1-14^{UGA} allele from yeast

Genomic DNA was prepared from yeast strain IS31Δ7b/1c as described previously (Hoffman & Winston, 1987). The *ade1-14* gene was PCR amplified from this strain using *Pfu* DNA polymerase (Stratagene) and standard protocols. PCR-amplified DNA was sequenced on both DNA strands.

ACKNOWLEDGMENTS

We thank Mick Tuite for the gift of anti-eRF3 antibody and plasmid pUKC 638 and Yuri Chernoff for strain GF417. Judith Bain, Carolina Ibanez, and Holger Pfrunder are thanked for providing able technical assistance. We are grateful to David Barford for sharing data with us in advance of publication and for helpful discussions. This research was supported by a Wellcome Trust grant to I.S. D.W.R. is supported by a Biotechnology and Biological Sciences Research Council grant (ref. 1/B10454).

Received April 11, 2000; returned for revision May 24, 2000; revised manuscript received June 22, 2000

REFERENCES

Alani E, Cao L, Kleckner N. 1987. A method for gene disruption that allows repeated use of *ura3* selection in the construction of multiply disrupted yeast strains. *Genetics 116*:541–545.

Bonetti B, Fu LW, Moon J, Bedwell DM. 1995. The efficiency of translation termination is determined by a synergistic interplay between upstream and downstream sequences in *Saccharomyces cerevisiae*. *J Mol Biol 251*:334–345.

Breining P, Piepersberg W. 1986. Yeast omnipotent suppressor *SUP1* (*SUP45*): Nucleotide sequence of the wild-type and a mutant gene. *Nucleic Acids Res 14*:5187–5197.

Brown CM, Tate WP. 1994. Direct recognition of mRNA stop signals by *Escherichia coli* polypeptide chain release factor two. *J Biol Chem 269*:33164–33170.

Chernoff YO, Vincent A, Liebman SW. 1994. Mutations in eukaryotic 18S ribosomal RNA affect translational fidelity and resistance to aminoglycoside antibiotics. *EMBO J 13*:906–913.

Cox BS. 1977. Allosuppressors in yeast. *Genet Res 30*:187–205.

Draper DE. 1999. Themes in RNA–protein recognition. *J Mol Biol 293*:255–270.

Eurwilaichitr L, Graves FM, Stansfield I, Tuite MF. 1999. The C-terminus of eRF1 defines a functionally important domain for translation termination in *Saccharomyces cerevisiae*. *Mol Microbiol 32*:485–496.

Finkelstein DB, Strausberg S. 1983. Heat shock regulated production of *E. coli* β-galactosidase in *Saccharomyces cerevisiae. Mol Cell Biol 3*:1625–1633.

Frolova L, Legoff X, Rasmussen HH, Cheperegin S, Drugeon G, Kress M, Arman I, Haenni AL, Celis JE, Philippe M, Justesen J, Kisselev L. 1994. A highly conserved eukaryotic protein family possessing properties of polypeptide-chain release factor. *Nature 372*:701–703.

Frolova L, Legoff X, Zhouravleva G, Davydova E, Philippe M, Kisselev L. 1996. Eukaryotic polypeptide-chain release factor eRF3 is an eRF1-dependent and ribosome-dependent guanosine triphosphatase. *RNA 2*:334–341.

Frolova LY, Tsivkovskii RY, Sivolobova GF, Oparina NY, Serpinsky OI, Blinov VM, Tatkov SI, Kisselev LL. 1999. Mutations in the highly conserved GGQ motif of class 1 polypeptide release factors abolish ability of human eRF1 to trigger peptidyl-tRNA hydrolysis. *RNA 5*:1014–1020.

Gietz RD, Woods RA. 1994. High efficiency transformation with lithium acetate. In: Johnston JR, ed. *Molecular genetics of yeast: A practical approach*. Oxford: IRL Press. pp 121–134.

Harlow E, Lane D. 1988. *Antibodies: A laboratory manual*. Cold Spring Harbor, New York: Cold Spring Harbor Laboratory Press.

Hawthorne DC, Leupold U. 1974. Suppressors in yeast. *Curr Top Microbiol Immunol 64*:1–47.

Hoffman CS, Winston F. 1987. A ten minute DNA preparation from yeast efficiently releases autonomous plasmids for transformation of *Escherichia coli*. *Gene 57*:267–272.

Ito K, Ebihara K, Nakamura Y. 1998. The stretch of C-terminal acidic amino acids of translational release factor eRF1 is a primary binding site for eRF3 of fission yeast. *RNA 4*:958–972.

Ito K, Ebihara K, Uno M, Nakamura Y. 1996. Conserved motifs in prokaryotic and eukaryotic polypeptide release factors—transfer-RNA-protein mimicry hypothesis. *Proc Natl Acad Sci USA 93*:5443–5448.

Ito K, Uno M, Nakamura Y. 2000. A tripeptide "anticodon" deciphers stop codons in messenger RNA. *Nature 403*:680–684.

Karamyshev AL, Ito K, Nakamura Y. 1999. Polypeptide release factor eRF1 from *Tetrahymena thermophila*: cDNA cloning, purification and complex formation with yeast eRF3. *FEBS Lett 457*:483–488.

Kuchino Y, Hanyu N, Tashiro F, Nishimura S. 1985. *Tetrahymena thermophila* glutamine tRNA and its gene that corresponds to UAA termination codon. *Proc Natl Acad Sci USA 82*:4758–4762.

Laemmli UK. 1970. Cleavage of structural proteins during the assembly of the head of bacteriophage T4. *Nature 227*:680–689.

Legoff X, Philippe M, JeanJean O. 1997. Overexpression of human release factor 1 alone was an antisuppressor effect in human cells. *Mol Cell Biol 17*:3164–3172.

Merkulova TI, Frolova LY, Lazar M, Camonis J, Kisselev LL. 1999. C-terminal domains of human translation termination factors eRF1 and eRF3 mediate their in vivo interaction. *FEBS Lett 443*:41–47.

Mottaguitabar S, Tuite MF, Isaksson LA. 1998. The influence of 5′ codon context on translation termination in *Saccharomyces cerevisiae*. *Eur J Biochem 257*:249–254.

Nicholls A, Sharp KA, Honig B. 1991. Protein folding and association—insights from the interfacial and thermodynamic properties of hydrocarbons. *Proteins Struct Funct Genet 11*:281–296.

Nissen P, Kjeldgaard M, Thirup S, Polekhina G, Reshetnikova L, Clark BF, Nyborg J. 1995. Crystal structure of the ternary complex of Phe-tRNAPhe, EF-Tu, and a GTP analog. *Science 270*:1464–1472.

Oubridge C, Ito N, Evans PR, Teo CH, Nagai K. 1994. Crystal-structure at 1.92 Ångstrom resolution of the RNA-binding domain of the U1a spliceosomal protein complexed with an RNA hairpin. *Nature 372*:432–438.

Poole ES, Major LL, Mannering SA, Tate WP. 1998. Translational termination in *Escherichia coli*: Three bases following the stop codon crosslink to release factor 2 and affect the decoding efficiency of UGA-containing signals. *Nucleic Acids Res 26*:954–960.

Rimmele ME, Belasco JG. 1998. Target discrimination by RNA-binding proteins: Role of the ancillary protein U2A′ and a critical leucine residue in differentiating the RNA-binding specificity of spliceosomal proteins U1A and U2B″. *RNA 4*:1386–1396.

Ritchie DW, Kemp GJL. 2000. Protein docking using spherical polar fourier correlations. *Proteins Struct Funct Genet 39*:178–194.

Sambrook J, Fritsch EF, Maniatis T. 1989. *Molecular cloning: A laboratory manual*. Cold Spring Harbor, New York: Cold Spring Harbor Laboratory Press.

Scolnick ER, Tompkins R, Caskey CT, Niremberg M. 1968. Release factors differing in specificity for terminator codons. *Proc Natl Acad Sci USA 61*:768–774.

Selmer M, Al Karadaghi S, Hirokawa G, Kaji A, Liljas A. 1999. Crystal structure *of Thermotoga maritima* ribosome recycling factor: A tRNA mimic. *Science 286*:2349–2352.

Sherman F, Hicks J 1991. Micromanipulation and dissection of asci. In: Guthrie CR, Fink GR, eds. *Methods in enzymology*. San Diego: Academic Press. pp 21–37.

Sikorski RS, Boeke JD 1991. In vitro mutagenesis and plasmid shuffling: From cloned gene to mutant yeast. In: Guthrie CR, Fink GR, eds. *Methods in enzymology*. San Diego: Academic Press. pp 302–318.

Sikorski RS, Hieter P. 1989. A system of shuttle vectors and yeast host strains designed for efficient manipulation of DNA in *Saccharomyces cerevisiae*. *Genetics 122*:19–27.

Song H, Mugnier P, Webb HM, Evans DR, Tuite MF, Hemmings BA, Barford D. 2000. The crystal structure of human eukaryotic release factor eRF1–mechanism of stop codon recognition and peptidyl-tRNA hydrolysis. *Cell 100*:311–321.

Stansfield I, Akhmaloka, Tuite MF. 1995b. A mutant allele of the *sup45* (*sal4*) gene of *Saccharomyces cerevisiae* shows temperature-dependent allosuppressor and omnipotent suppressor phenotypes. *Curr Genet 27*:417–426.

Stansfield I, Eurwilaichitr L, Akhmaloka, Tuite MF. 1996. Depletion in the levels of the release factor eRF1 causes a reduction in the efficiency of translation termination in yeast. *Mol Microbiol 20*:1135–1143.

Stansfield I, Grant CM, Akhmaloka, Tuite MF. 1992. Ribosomal association of the yeast *sal4* (*sup45*) gene-product—implications for its role in translation fidelity and termination. *Mol Microbiol 6*:3469–3478.

Stansfield I, Jones KM, Kushnirov VV, Dagkesamanskaya AR, Poznyakovski AI, Paushkin SV, Nierras CR, Cox BS, Teravanesyan MD, Tuite MF. 1995a. The products of the *SUP45* (eRF1) and *SUP35* genes interact to mediate translation termination in *Saccharomyces cerevisiae*. *EMBO J 14*:4365–4373.

Thompson JD, Higgins DG, Gibson TJ. 1994. CLUSTAL W: Improving the sensitivity of progressive multiple sequence alignment through sequence weighting, position-specific gap penalties, and weight matrix choice. *Nucl Acids Res 22*:4673–4680.

Weiss RB, Murphy JP, Gallant JA. 1984. Genetic screen for cloned release factor genes. *J Bacteriol 158*:362–364.

Zhouravleva G, Frolova L, Legoff X, Leguellec R, Ingevechtomov S, Kisselev L, Philippe M. 1995. Termination of translation in eukaryotes is governed by 2 interacting polypeptide-chain release factors, eRF1 and eRF3. *EMBO J 14*:4065–4072.